

**SYNTHESIS AND CHARACTERIZATION OF  
ORGANIC-INORGANIC BISMUTH HALIDE  
PEROVSKITES FOR PHOTONICS APPLICATIONS**

**HENG HAN YANN**

**UNIVERSITI SAINS MALAYSIA**

**2023**

**SYNTHESIS AND CHARACTERIZATION OF  
ORGANIC-INORGANIC BISMUTH HALIDE  
PEROVSKITES FOR PHOTONICS APPLICATIONS**

by

**HENG HAN YANN**

**Thesis submitted in fulfilment of the requirements  
for the degree of  
Doctor of Philosophy**

**September 2023**

## ACKNOWLEDGEMENT

I would like to take this opportunity to express my heartfelt gratitude to all those who have contributed to the successful completion of my dissertation. I couldn't achieve my ambition without the assist of people around me.

First and foremost, I am grateful to my supervisor, Dr. Mundzir Abdullah from INOR, for his invaluable guidance, support, and Ministry of Higher Education Malaysia for the 2.4-year FRGS that made this research possible.

I am thankful to my co-supervisors, Prof. Dr. Abdul Razak Ibrahim from the Crystallography Lab for his advice and support. Without an equipped laboratory, I will not be able to conduct research experiment with ease. Same to Dr. Shuaib Saheed from UTP for his advice which helped me improve my experiment and dissertation.

I would like to extend my thanks to all staff from X-ray lab, NOR lab, INOR lab, SERC, School of Chemical Sciences, School of Biological Sciences, and School of Physics. Without their advice and support on characterization tests, I would not able to finish my research work on time. Especially to: Dr. Suhana Arshad, Dr. Mohd. Mustaqim Rosli, En. Noor Aswafi Ahmad Zaini, Dr. Dian Alwani Zainuri, Mohd. Mustaqim Abu Bakar, Dr. Mohd Marzaini Mohd Rashid, En. Abdul Jamil Yusuf, Pn. Ng Bee Choo, Pn. Aznorhaida Ramli, En. Yushamdan Yusof, Pn. Mahfuzah Mohamad Fuad, Dr. Sabah Mohammad, Cik Rahmahwatini Abd Rahman, Prof. Madya. Dr. Naser Mahmoud Ahmed, En. Mohd Zharif Ahmad Thirmizir, En. Mohd Azrul Abd Aziz, Dr. Mohammad Anwar Mohamed Iqbal, Dr. Mohd Rizal Razali, En. Azhar Ramli Harun, En. Masrol Mansor and Cik Izzati Zahidah.

I would like to express my appreciation to all staff from USM, INOR, IPS, Nerve Centre, Bakti Fajar Hostel (H51) and Engineering Library, who helped me directly or

indirectly. Especially to En. Wan Rosdan Rozali for his assistance in arranging all the study-related matters. Extremely grateful to Cik Junainah Abu Seman and Cik Jamilah Hassan Basri who help me to arrange the back-up laptop for my VIVA presentation.

Special thanks to my lab mates, Muhamad Fikri Zaini, Ainizatul Husna Anizaim, Samuel Obaseki (Nigeria), Dr. Halo Dalshad Omar (Kazakhstan), and Saleh Alsaee for their comments and suggestions. Especially to Mohamad Aizat Abu Bakar for aiding and teaching me on nonlinear optics and Wong Qin Ai for coaching me the single crystal data interpretation. Not to forget Rebecca Leong from UTP for her coaching in synthesising perovskites. Thanks for encouragement from Nor-lab mates Dr. Wang Tian Kun, Ainita Rozati, Puteri Haslinda, Dr. Lau Khai Shenn, Abed Shireen, Dr. Muhammad Aminu, Mohd Ann Amirul Zulffiqal, and Ahlaam Taher.

I am deeply grateful to all the manuscripts reviewers who took the time to check and give their opinions on my manuscripts. Their feedback provided me with room for improvement and additional knowledge to better understand my research work.

I am also grateful to my friends: Ms. Wong Shyu Jeng, Ms. Wai Poh Choo, Ms. Fong Li Fung, Dr. Wan Rosmiza Zana, Mr. Dennis Chin, Mr. Chuah Tong Hock and Mr. Kasem Bau, for their motivation and support during the COVID-19 period.

Finally, I would like to thank my beloved family, especially my mom Zhen, dad Zhen Yu, aunty Fang, uncle Nam, sis Wei, brother Yao and Qing, for their unwavering love and support. Also, I would like to express my gratitude to my dearly missed late grandma Xiu Fong, grandpa Zhong Ting, uncle Liang, and aunty Chong Chui Zhen for their constant love and encouragement while they were still alive.

Thank you all once again for your invaluable support, encouragement, and guidance throughout my four-year research journey.

## TABLE OF CONTENTS

<b>ACKNOWLEDGEMENT</b> .....	<b>ii</b>
<b>TABLE OF CONTENTS</b> .....	<b>iv</b>
<b>LIST OF TABLES</b> .....	<b>viii</b>
<b>LIST OF FIGURES</b> .....	<b>ix</b>
<b>LIST OF SYMBOLS</b> .....	<b>xiv</b>
<b>LIST OF ABBREVIATIONS</b> .....	<b>xv</b>
<b>LIST OF APPENDICES</b> .....	<b>xvii</b>
<b>ABSTRAK</b> .....	<b>xviii</b>
<b>ABSTRACT</b> .....	<b>xx</b>
<b>CHAPTER 1 INTRODUCTION</b> .....	<b>1</b>
1.1 Perovskites as nonlinear optical material .....	1
1.2 Problem Statements .....	5
1.3 Research Questions .....	7
1.4 Research Objectives .....	8
1.5 Novelty of the research work .....	8
1.6 Research Scope .....	9
1.7 Thesis outline .....	10
<b>CHAPTER 2 LITERATURE REVIEW AND THEORY</b> .....	<b>12</b>
2.1 Introduction .....	12
2.2 Halide Perovskite – three-dimensional (3D) - zero-dimensional (0D) .....	12
2.3 Drawbacks of Perovskites .....	19
2.4 Toxicological research of lead (Pb) - based perovskite .....	22
2.5 Hybrid bismuth (Bi) - based halide perovskite .....	25
2.6 Overview of perovskites synthesis approach .....	26
2.6.1 A site organic cation of reagent.....	28

2.6.2	Ligands .....	29
2.6.3	Solvents .....	30
2.6.4	Heat setting.....	33
2.6.5	Solution-based perovskites.....	34
2.6.6	Summary of perovskite synthesis approaches.....	35
2.7	Overview of nonlinear optics (NLO) .....	36
2.7.1	2 <sup>nd</sup> order nonlinear optics (NLO) .....	40
2.7.2	3 <sup>rd</sup> order nonlinear optics (NLO).....	40
2.7.3	z-scan theory .....	41
2.7.4	Optical limiting (OL) concept .....	46
2.7.5	Summary of nonlinear optics (NLO) phenomena .....	48
2.8	Conventional nonlinear optics (NLO) materials .....	49
2.9	Quantum dots (QDs) perovskites as a nonlinear optics (NLO) material .....	51
2.10	Potential photonics applications of perovskites quantum dots (QDs).....	54
<b>CHAPTER 3 METHODOLOGY.....</b>		<b>56</b>
3.1	Introduction .....	56
3.2	Preparation of samples study.....	57
3.2.1	List of chemicals .....	57
3.2.2	Synthesis of colloidal quantum dots (QDs) solutions .....	60
3.2.3	Preparation of thin film and powder sample .....	64
3.2.4	Preparation of PhA <sub>4</sub> BiI <sub>6</sub> Single Crystal .....	64
3.3	Single Crystal X-ray diffractometer (SC-XRD).....	65
	3.3.1 (a) X-ray structure determination.....	65
	3.3.1 (b) Theoretical calculation.....	66
3.4	Spectroscopy Studies.....	67
3.4.1	Ultraviolet-Visible (UV-vis) spectroscopy .....	67
	3.4.1 (a) Tauc plot from UV-vis data.....	68

3.4.1 (b)	Criteria for measuring stability of perovskites .....	69
3.4.2	Photoluminescence (PL) spectroscopy.....	70
3.4.3	Fourier transform infrared (FTIR) spectroscopy.....	70
3.4.4	Luminescence chromaticity.....	71
3.5	Imaging and structural studies.....	72
3.5.1	Field emission scanning electron microscopy with energy dispersive x-ray spectroscopy (FESEM-EDX) .....	72
3.5.2	High-resolution transmission electron microscopy (HRTEM) .....	72
3.5.3	X-ray powder diffraction (XRD).....	73
3.5.4	Atomic force microscopy (AFM).....	74
3.6	Nonlinear optics (NLO) and optical limiting (OL) studies .....	74
3.6.1	z-scan technique .....	74
3.6.2	Optical limiting effect (OL) .....	76
<b>CHAPTER 4 RESULTS AND DISCUSSIONS .....</b>		<b>77</b>
4.1	Introduction .....	77
4.2	Sample labelling in this study .....	78
4.3	X-ray crystallographic analysis of PhA <sub>4</sub> BiI <sub>6</sub> single crystal. ....	80
4.4	Stability study for PhA <sub>4</sub> BiX <sub>6</sub> quantum dots (QDs) samples .....	92
4.4.1	Optical bandgap calculated by Tauc plot .....	105
4.5	Linear optical properties study .....	107
4.6	Luminescence chromaticity study .....	111
4.7	Structure and surface morphology analysis.....	114
4.8	Third order nonlinear optics (NLO) characterizations for all samples .....	124
4.9	Optical limiting (OL) performance .....	149
<b>CHAPTER 5 CONCLUSIONS AND FUTURE RECOMMENDATIONS .</b>		<b>159</b>
5.1	Conclusions .....	159
5.2	Recommendations for Future Research .....	163

**REFERENCES..... 165**

**APPENDICES**

**LIST OF PUBLICATIONS**



## LIST OF TABLES

		<b>Page</b>
Table 2.1	Summary of techniques to prepare Pb-free hybrid perovskites. ....	27
Table 2.2	Polar and non-polar solvents with each boiling point and dielectric .....	32
Table 2.3	NLO respond of traditional NLO materials. ....	50
Table 3.1	List of chemicals used in the study. ....	58
Table 3.2	Solubility of reagents. ....	59
Table 3.3	z-scan parameters. ....	76
Table 4.1	27 samples preparation detail with labelling in this study. ....	79
Table 4.2	Crystal data and structure refinement details for TIHM. ....	82
Table 4.3	Bond length and bond angle comparison between X-ray experiment and theoretical parameters for Bi-I interactions. ....	83
Table 4.4	The geometry of hydrogen-bonding ( $^{\circ}\text{A}$ , $^{\circ}$ ) of the crystal. ....	85
Table 4.5	Experimental and calculated values by TD-DFT at B3LYP by level of theory. ....	90
Table 4.6	The calculated field independent dipole moment for TIHM. ....	92
Table 4.7	Summarization of the optical properties of $\text{PhA}_4\text{BiX}_6$ . ....	110
Table 4.8	Comparison $\chi^{(3)}$ NLO parameter of $\text{PhA}_4\text{BiX}_6$ (X= I, Br, Cl) with different synthesis parameter. ....	129
Table 4.9	3 <sup>rd</sup> order NLO parameters under the 637 nm laser excitation. ....	144
Table 4.10	Comparison of NLO parameters with the other reported other perovskites materials by z-scan technique. ....	148
Table 4.11	Summary of evaluated OL threshold at 808 nm for each QDs sample. ....	157
Table 4.12	The OL performance of the $\text{PhA}_4\text{BiX}_6$ QDs and reported perovskites. ....	158

## LIST OF FIGURES

		<b>Page</b>
Figure 1.1	NLO study of perovskite publications for the past 8 years. Searched terms: " perovskite " and "nonlinear optics " (Source: Web of Science Core Collection only from January 2015 to February 2023).....	3
Figure 1.2	Nonlinear optical materials market by product type (second order nonlinearity and third order nonlinearity) for electronics, automotive and aerospace applications from 2019-2027 (Profshare Market Research, 2019). ....	5
Figure 2.1	Single unit cell of an ABX <sub>3</sub> perovskite crystal (Tan <i>et al.</i> , 2014).....	13
Figure 2.2	Different metal halide perovskite crystal structures of 3D cubic-phase AMX <sub>3</sub> , 2D A <sub>2</sub> MX <sub>4</sub> , 2D A <sub>3</sub> M <sub>2</sub> X <sub>9</sub> , 2D AM <sub>2</sub> X <sub>5</sub> , 0D A <sub>4</sub> MX <sub>6</sub> , and 3D double perovskites A <sub>2</sub> MM <sub>0</sub> X <sub>6</sub> (Bhaumik <i>et al.</i> , 2020).....	14
Figure 2.3	Types of connectivity BX <sub>6</sub> octahedra in perovskite-like halides (Song <i>et al.</i> , 2019).....	15
Figure 2.4	Energy band gap versus perovskite dimension (Han <i>et al.</i> , 2020)....	17
Figure 2.5	The degree of confinement for different structure of materials. (Edvinsson, 2018). ....	18
Figure 2.6	Stability issues in perovskites and perovskites solar cells (Mazumdar <i>et al.</i> , 2021).....	20
Figure 2.7	Pb-free Perovskite QDs publication. Searched terms: "perovskite", "quantum dot" and "lead-free " (Source: Web of Science Core Collection only from January 2016 to February 2023).....	22
Figure 2.8	Absorption and PL spectra for MA <sub>3</sub> Bi <sub>2</sub> X <sub>9</sub> QDs by halide substitution (left to right Cl, Br, and I) (Leng <i>et al.</i> , 2016).....	30
Figure 2.9	Structure of different solvent and the categories of hazardous (Gardner <i>et al.</i> , 2016).....	31
Figure 2.10	Solid state ligand exchange (top) and solution-phase exchange.....	35
Figure 2.11	Linear (a) and (b) NLO effects (Vasconcelos, 2022).....	37
Figure 2.12	Nonlinear optics applications (Garmire, 2013).....	38
Figure 2.13	The differences between linear and nonlinear induced polarization: (a) linear dependence holds for a low input field. (b) nonlinear induced polarization by inputting a high electric (HC Photonics Corp, 2017). ....	39
Figure 2.14	SHG of (a) Geometry (left) and energy-level diagram (right) (Boyd, 2020), (b) Wavelength conversion (Vabishchevich <i>et al.</i> , 2018) . ....	40

Figure 2.15	(a) Sample at the focal point ( $z = 0$ ), (b) sample self-focusing ( $+n_2$ ), and (c) sample self-defocusing ( $-n_2$ ) (Pandiyan <i>et al.</i> , 2020).....	43
Figure 2.16	Principle of absorption (Karuppasamy <i>et al.</i> , 2018).....	44
Figure 2.17	The response of an optical limiter by input fluence or energy versus transmittance. ....	47
Figure 2.18	Various mechanisms responsible for OL (Polavarapu, 2011).....	47
Figure 2.19	Energy band structures in atom, QDs, quantum nanostructure and bulk semiconductors (Blood, 2015; Ramalingam, 2020).....	53
Figure 3.1	Flow of research study. ....	57
Figure 3.2	Chemical structure of phenyammonium halide (I/Br/Cl). ....	59
Figure 3.3	Chemical structure of Bi halide (I/Br/Cl).....	59
Figure 3.4	Samples preparation flow for $\text{PhA}_4\text{BiI}_6$ and $\text{PhA}_4\text{BiBr}_6$ group. ....	60
Figure 3.5	Samples preparation flow for $\text{PhA}_4\text{BiCl}_6$ .....	61
Figure 3.6	Process flow to prepare $\text{PhA}_4\text{BiI}_6$ , and $\text{PhA}_4\text{BiBr}_6$ samples for OSS and non-coordinate solvent method: (a) weighing of reagents, (b) addition of solvent, (c) stirring, (d) precursor mixing with toluene, (e) pouring into a centrifuge tube, (f) centrifugation, and (g) filtration.....	62
Figure 3.7	Process flow to prepare $\text{PhA}_4\text{BiI}_6$ , and $\text{PhA}_4\text{BiBr}_6$ samples for OSS + OA method: (a) weighing of reagents, (b) addition of solvent, (c) stirring, (d) mixing toluene with OA, (e) precursor mixing with toluene + OA, (f) pouring into a centrifuge tube, (g) centrifugation, and (h) filtration. ....	63
Figure 3.8	Thin film preparation process: (a) drop-cast, (b) spin-coat, and (c) drying. ....	64
Figure 3.9	Steps to grow a single crystal: (a) weighing reagents, (b) adding solvent, (c) stirring with heating, (d) pouring into a vial, (e) sealing with parafilm picked with small holes, and (f) single crystal obtained. ....	65
Figure 3.10	Criteria for degradation of the samples used in this study. ....	69
Figure 3.11	Spectroradiometer device set up. ....	71
Figure 3.12	Lacey carbon supported copper grid (Sigma-Aldrich) (left) and.....	73
Figure 3.13	z-scan set up. ....	75
Figure 3.14	Experimental set up for optical limiting study.....	76
Figure 4.1	Front view (left) and top view (right). ....	80
Figure 4.2	A unit cell of single crystal TIHM perovskite. ....	80
Figure 4.3	ORTEP diagram (left) and optimized structure of TIHM (right). ....	81
Figure 4.4	Hydrogen-bonding network (dash line of TIHM compound) viewed down $a$ -axis.....	84
Figure 4.5	Alternating layers of TIHM compound.....	85

Figure 4.6	(a) The symmetry operation and structural view along the <i>b</i> -axis distinguish the TIHM crystal packing diagram (b) and <i>c</i> -axis. (Hydrogen atoms are omitted for clarity).....	86
Figure 4.7	The Hirshfeld surfaces mapped with $d_{\text{norm}}$ and overall fingerprints for (a) the asymmetric unit, (b) $[\text{BiI}_6]^{3+}$ - octahedral, (c) $[(\text{C}_6\text{H}_5)\text{NH}_3]^+$ cations, (d) $\text{I}^-$ anion and (e) water molecule $\text{H}_2\text{O}$ display the total Hirshfeld surface provided by each interaction.....	89
Figure 4.8	The (a) experimental (inset bandgap calculation) and (b) UV-vis absorption spectra of TIHM (theoretical). .....	90
Figure 4.9	The frontier molecular orbitals plots (HOMO and LUMO) of TIHM compound at DFT/B3LYP/6-311++G(d,p) + LanL2DZ basis set level with the energy band gap. ....	90
Figure 4.10	Theoretical molecular electrostatic potential surface of (a) TIHM and individual molecules, i.e., (b) iodidebismuthate, (c) phenylammonium, (d) water and (e) iodide anion. (isovalue = 0.001 a.u.). The electric dipole moment is showed as blue vector. ...	92
Figure 4.11	UV-vis absorption spectrum of colloidal $\text{PhA}_4\text{BiI}_6$ prepared with EtOH at (a) 25 °C, (b) 60 °C and (c) 100 °C with Tauc analysis of each absorption spectra (right).....	94
Figure 4.12	UV-vis absorption spectra of colloidal $\text{PhA}_4\text{BiI}_6$ prepared with EtOH + OA at (a) 25 °C, (b) 60 °C and (c) 100 °C with Tauc analysis of each absorption spectra (right).....	95
Figure 4.13	UV-vis absorption spectra of colloidal $\text{PhA}_4\text{BiI}_6$ prepared with GBL at at (a) 25 °C, (b) 60 °C and (c) 100 °C with Tauc analysis of each absorption spectra (right).....	96
Figure 4.14	UV-vis absorption spectra of colloidal $\text{PhA}_4\text{BiBr}_6$ prepared with EtOH at (a) 25 °C, (b) 60 °C and (c) 100 °C with Tauc analysis of each absorption spectra (right).....	97
Figure 4.15	UV-vis absorption spectra of colloidal $\text{PhA}_4\text{BiBr}_6$ prepared with EtOH + OA at (a) 25 °C, (b) 60 °C and (c) 100 °C with Tauc analysis of each absorption spectra (right).....	98
Figure 4.16	UV-vis absorption spectra of colloidal $\text{PhA}_4\text{BiBr}_6$ prepared with GBL at (a) 25 °C, (b) 60 °C and (c) 100 °C with Tauc analysis of each absorption spectra (right).....	99
Figure 4.17	UV-vis absorption spectra of colloidal $\text{PhA}_4\text{BiCl}_6$ prepared with DMSO solvent at (a) 25 °C, (b) 60 °C and (c) 100 °C with Tauc analysis of each absorption spectra (right).....	100
Figure 4.18	UV-vis absorption spectra of colloidal $\text{PhA}_4\text{BiCl}_6$ prepared with DMSO solvent added OA at (a) 25 °C, (b) 60 °C and (c) 100 °C with Tauc analysis of each absorption spectra (right).....	100
Figure 4.19	UV-vis absorption spectrum of colloidal $\text{PhA}_4\text{BiCl}_6$ prepared by GBL solvent at 25 °C (top), 60 °C (middle) and 100 °C (bottom) with Tauc analysis of each absorption spectra. ....	102

Figure 4.20	Stability analysis of the samples summarized based on criteria 1 and.....	104
Figure 4.21	Illustration direct energy bandgap value of each the $\text{PhA}_4\text{BiX}_6$ .....	106
Figure 4.22	UV-vis absorption spectra and emission spectra for (a) $\text{PhA}_4\text{BiI}_6$ QDs (EtOH + OA, 60 °C) (b) $\text{PhA}_4\text{BiBr}_6$ (EtOH + OA, 60 °C) QDs, (c) $\text{PhA}_4\text{BiCl}_6$ (DMSO + OA, 60 °C) QDs.....	109
Figure 4.23	Blue emission of $\text{PhA}_4\text{BiCl}_6$ (DMSO, 100°C) after 50 weeks.....	112
Figure 4.24	Emission photographs solutions under UV-390 nm laser excitation and colour purity of (a) $\text{PhA}_4\text{BiI}_6$ , (b) $\text{PhA}_4\text{BiBr}_6$ , and (c) $\text{PhA}_4\text{BiCl}_6$ QDs solutions.....	113
Figure 4.25	FTIR spectra for $\text{PhA}_4\text{BiI}_6$ QDs. Insets show the structure of the ionic compound between $\text{PhA}^+$ and $\text{BiI}_6^{3-}$ .....	115
Figure 4.26	FTIR spectra for $\text{PhA}_4\text{BiBr}_6$ QDs. Insets show the structure of the ionic compound between $\text{PhA}^+$ and $\text{BiBr}_6^{3-}$ .....	115
Figure 4.27	FTIR spectra for $\text{PhA}_4\text{BiCl}_6$ QDs. Insets show the structure of the ionic compound between $\text{PhA}^+$ and $\text{BiCl}_6^{3-}$ .....	116
Figure 4.28	EDX profile analysis for (a) $\text{PhA}_4\text{BiI}_6$ , (b) $\text{PhA}_4\text{BiBr}_6$ , and (c) $\text{PhA}_4\text{BiCl}_6$ . Inset: the top view FESEM image of each sample on a micrometer scale.....	118
Figure 4.29	HRTEM image of $\text{PhA}_4\text{BiI}_6$ QDs (a) at scale bar 100 nm (b) an isolated perovskite nanoparticle at scale bar 5 nm and (c) lattice spacing, crystal plane and Fourier transform (FFT) pattern of (b) (inset).....	119
Figure 4.30	HRTEM image of $\text{PhA}_4\text{BiBr}_6$ QDs (a) at scale bar 100 nm (b) an isolated perovskite nanoparticle at scale bar 5 nm and (c) lattice spacing, crystal plane and Fourier transform (FFT) pattern of (b) (inset).....	120
Figure 4.31	HRTEM image of $\text{PhA}_4\text{BiCl}_6$ QDs (a) at scale bar 100 nm (b) an isolated perovskite nanoparticle at scale bar 5 nm and (c) lattice spacing, crystal plane and Fourier transform (FFT) pattern of (b) (inset).....	120
Figure 4.32	Size distribution histogram of (a) $\text{PhA}_4\text{BiI}_6$ , (b) $\text{PhA}_4\text{BiBr}_6$ , and (c) $\text{PhA}_4\text{BiCl}_6$ QDs, calculated using a minimum of 70 nanoparticles....	121
Figure 4.33	Powder XRD measurements of (a) $\text{PhA}_4\text{BiI}_6$ (EtOH, 60 °C), (b) $\text{PhA}_4\text{BiBr}_6$ (EtOH, 60 °C), and (c) $\text{PhA}_4\text{BiCl}_6$ (DMSO, 60 °C) refer to (d) $\text{PhA}_4\text{BiI}_6$ single crystal powder pattern reported in CCDC 2071510. The $\text{PhA}_4\text{BiX}_6$ (X = I, Br, Cl) sharing similar crystal structure.....	123
Figure 4.34	AFM topology for (a) $\text{PhA}_4\text{BiI}_6$ , (b) $\text{PhA}_4\text{BiBr}_6$ , and (c) $\text{PhA}_4\text{BiCl}_6$ .....	124
Figure 4.35	$n_2$ and $\beta$ NLA for each sample which prepared at 60 °C correspond to the $E_g$ .....	145

Figure 4.36	OL action for $\text{PhA}_4\text{BiI}_6$ prepare with EtOH only at different temperatures, (a) 25 °C, (b) 60 °C and (c) 100 °C. ....	151
Figure 4.37	OL action for $\text{PhA}_4\text{BiI}_6$ prepare with EtOH + OA at different temperatures, (a) 25 °C, (b) 60 °C and (c) 100 °C. ....	151
Figure 4.38	OL action for $\text{PhA}_4\text{BiI}_6$ prepare with GBL at different temperatures, (a) 25 °C, (b) 60 °C and (c) 100 °C. ....	152
Figure 4.39	OL for action $\text{PhA}_4\text{BiBr}_6$ prepare with EtOH only at different temperatures, (a) 25 °C, (b) 60 °C and (c) 100 °C. ....	152
Figure 4.40	OL action for $\text{PhA}_4\text{BiBr}_6$ prepare with EtOH + OA at different temperatures, (a) 25 °C, (b) 60 °C and (c) 100 °C. ....	153
Figure 4.41	OL action for $\text{PhA}_4\text{BiBr}_6$ prepare with GBL at different temperatures, (a) 25 °C, (b) 60 °C and (c) 100 °C. ....	153
Figure 4.42	OL action for $\text{PhA}_4\text{BiCl}_6$ prepare with DMSO at different temperatures, (a) 25 °C, (b) 60 °C and (c) 100 °C. ....	154
Figure 4.43	OL action for $\text{PhA}_4\text{BiCl}_6$ prepare with DMSO + OA at different temperatures, (a) 25 °C, (b) 60 °C and (c) 100 °C. ....	154
Figure 4.44	OL action for $\text{PhA}_4\text{BiCl}_6$ prepare with GBL at different temperatures, 25 °C (left), 60 °C (right) and 100 °C (bottom). ....	155
Figure 4.45	$L_{\text{th}}$ and $L_{\text{on}}$ for all samples synthesized with different methods and different temperatures (25 °C, 60 °C, and 100 °C). ....	156

## LIST OF SYMBOLS

$\beta$	Nonlinear absorption coefficient
$Im$	Imaginary parts
$n_2$	Nonlinear refractive index
$Re$	Real parts
$\chi^{(3)}$	Third order susceptibility
$E$	Electric field
$L_{th}$	Optical limiting threshold
$L_{on}$	Optical limiting onset
$P$	Polarization
$\lambda_{peak}$	Peak absorption wavelength
$\alpha$	Linear absorption coefficient
$L_{eff}$	Effective thickness
$\omega_0$	Gaussian beam waist radius
$I_0$	Intensity at the focus
$k$	Wave vector
$\epsilon_0$	Permittivity of free space
$c$	Speed of light
$\mathcal{E}$	Field amplitude
$n_0$	Refractive index
$\lambda$	Wavelength
$h$	Planck's constant
$\nu$	Frequency of incident photons
$P_L$	Linear polarization
$\omega$	Light frequency
$d_{norm}$	Contact distance
$d_i$	Distance to the nearest nucleus internal to the surface
$d_e$	Distance from the point to the nearest nucleus external
$r_i^{vdw}$	vdw radius of the internal to the surface
$r_e^{vdw}$	vdw radius of the external to the surface.
$\mu$	Dipole moment

## LIST OF ABBREVIATIONS

0D	Zero-dimensional
1D	One-dimensional
2D	Two-dimensional
3D	Three-dimensional
AFM	Atomic force microscopy
B3LYP	Becke's nonlocal three parameter exchange and the Lee, Young and Parr
BiBr <sub>3</sub>	Bismuth tribromide
BiCl <sub>3</sub>	Bismuth trichloride
BiI <sub>3</sub>	Bismuth triiodide
BiX	Bismuth halide
BBO	Beta barium borate
CCT	Colour temperature
CIE	Commission International de l'Eclairage
CIF	Crystallographic information file
DFT	Density functional theory
DMSO	Dimethyl sulfoxide
EL	Electroluminescence
EtOH	Ethanol
GaAs	Gallium arsenide
FESEM- EDX	Field emission scanning electron microscopy with energy-dispersive X- ray
FTIR	Fourier transform infrared
GaP	Gallium phosphide
GaN	Gallium nitride
GBL	$\gamma$ -butyrolactone
HOMO	Highest occupied molecular orbital
HRTEM	High-resolution transmission electron microscopy
KDNB	Potassium 3,5-dinitrobenzoate
KDP	Potassium dihydrogen phosphate
KNbO <sub>3</sub>	Potassium niobate



LARP	Ligand-assisted reprecipitation
LiNbO <sub>3</sub>	Lithium niobate
LED	Light-emitting diode
LUMO	Lowest unoccupied molecular orbital
MEtOH	Methanol
NLA	Nonlinear absorption
NLO	Nonlinear optics
NLR	Nonlinear refraction
OA	Oleic acid
OL	Optical limiting
ORTEP	Oak ridge thermal ellipsoid plot
OSS	One step solvent
RMS	Root means square
PhA <sub>4</sub> BiBr <sub>6</sub>	Phenylammonium bismuth bromide
PhA <sub>4</sub> BiCl <sub>6</sub>	Phenylammonium bismuth chloride
PhA <sub>4</sub> BiI <sub>6</sub>	Phenylammonium bismuth iodide
PhABr	Phenylammonium bromide
PhACl	Phenylammonium chloride
PhAI	Phenylammonium iodide
PhAX	Phenylammonium halide
PL	Photoluminescence
QDs	Quantum Dots
RSA	Reverse saturation absorption
SA	Saturation absorption
SHG	Second harmonic generation
SC-XRD	Single Crystal X-ray diffractometer
TIHM	Tetrakis(phenylammonium) iodide hexaiodidebismuthate monohydrate
TD-DFT	Time dependent density functional theory
TPA	Two-photon absorption
UV-vis	Ultraviolet visible
vdw	van der Waals
XRD	X-ray diffraction
ZnO	Zinc oxide

## LIST OF APPENDICES

Appendix A	Reagents information.
Appendix B	UV-vis absorbance for each reactant.
Appendix C	Estimation cost of each precursor solutions.
Appendix D	Solubility of precursor solution in different solvent.
Appendix E	List of preliminary trials to synthesize precursor solutions.
Appendix F	List of trials to synthesize single crystals by using solvent evaporation technique.
Appendix G	UV-vis stability monitoring for all samples.
Appendix H	Characterization test equipment.
Appendix I	z-scan setup at School of Physics, USM.
Appendix J	Experiment information.

**SINTESIS DAN PENCIRIAN**  
**PEROVSKIT BISMUT HALIDA ORGANIK-TAK ORGANIK**  
**UNTUK APLIKASI FOTONIK**

**ABSTRAK**

Kajian ini memberi tumpuan kepada sintesis sebatian perovskit Bi-halida organik-tidak organik menggunakan pelbagai halida (iodida, bromida, dan klorida) dengan cara yang rendah toksik dan mesra alam. Matlamatnya adalah untuk menghasilkan bahan perovskit yang bebas Pb yang selamat untuk pekerja dalam industri fotonik dan dapat dihasilkan kos rendah serta proses yang kurang rumit. Dalam konteks ini, kation phenylammonium hidrofobik ( $[(C_6H_5)NH_3]^+$ ) telah dipilih, dimana yang telah diketahui dapat menyumbang kepada kestabilan sampel yang lebih baik. Kaedah sintesis melibatkan tiga pendekatan berbeza: pelarut satu langkah (OSS), OSS tambahan asid oleik (OA), dan kaedah pelarut tanpa koordinasi pada suhu yang berbeza. Kestabilan sampel dinilai, dan didapati sampel yang disintesis pada suhu 60 °C menunjukkan kestabilan terbaik untuk kebanyakan pelarut dan jenis halida. Interaksi ion yang kuat antara anion  $BiX_6^{3-}$  dan kation  $PhA^+$  pendek dalam struktur 0D banyak menyumbang kepada kestabilannya. Secara umumnya, sampel  $PhA_4BiCl_6$  menunjukkan kestabilan tertinggi di kalangan halida berikutan tarikan yang lebih kuat antara nukleus dan elektron. Kajian ini juga melibatkan pertumbuhan hablur tunggal  $PhA_4BiI_6$  menggunakan teknik penyejatan pelarut di mana struktur sebatian perovskit dimensi sifar (0D) ditentukan, yang disokong oleh keputusan mikroskop imbasan elektron medan pelepasan dengan penyebaran tenaga sinar-X (FESEM-EDX), dan spektroskopi inframerah jelmaan Fourier (FTIR). Teknik mikroskopi seperti mikroskop elektron penghantaran resolusi tinggi (HRTEM) dan mikroskop daya atom

(AFM) digunakan untuk menganalisis struktur dan mempamerkan titik kuantum (QDs) dengan saiz kurang daripada 10 nm. Jurang jalur tenaga berbeza antara sampel halida yang dihasilkan, menjadikannya sesuai untuk aplikasi fotonik seperti LED, laser, dan peranti lain. Sampel menunjukkan penyinaran puncak dan tingkap ketelusan yang berbeza, menjadikannya sesuai untuk pelbagai aplikasi dalam pencahayaan dan fotonik. Sifat optik tak linear (NLO) dikaji menggunakan pengukuran z-scan, dan sampel menunjukkan fenomena nyahfokus sendiri dan penyerapan boleh tepu terbalik (RSA). Semakin besar saiz perovskit  $\text{PhA}_4\text{BiX}_6$  (berdasarkan halida dari Cl ke I), semakin kuat pembelauan tak linear (NLR) sebagaimana yang ditunjukkan oleh magnitud yang lebih tinggi bagi  $n_2$  dan  $\text{Re } \chi^{(3)}$ . Tambahan pula, sampel menunjukkan fenomena pembatasan optik (OL) dengan penyerapan linear diikuti oleh kepupusan tak linear melebihi nilai ambang. Mekanisme OL dikenalpasti sebagai jenis penyebaran tenaga dengan mekanisme penumpalan sendiri yang disokong oleh penyerakan tak linear panas pada partikel QDs hasil daripada interaksi laser gelombang berterusan. Sampel  $\text{PhA}_4\text{BiI}_6$  menunjukkan kuasa ambang OL tertinggi dan dianggap sebagai bahan yang berpotensi dan selamat untuk aplikasi laser kuasa tinggi dan pengimej biologi. Secara keseluruhannya, bahan perovskit bebas Pb yang disintesis menunjukkan potensi untuk aplikasi dalam platform fotonik tak linear, sumber cahaya, pengesan, fosfor dan pembatasan optik, terutamanya dalam teknik pengimejan biologi lanjutan yang memerlukan bahan bukan toksik.

**SYNTHESIS AND CHARACTERIZATION OF  
ORGANIC-INORGANIC BISMUTH HALIDE PEROVSKITES  
FOR PHOTONICS APPLICATIONS**

**ABSTRACT**

The study focused on synthesizing organic-inorganic Bi-halides perovskite compounds using different halides (iodide, bromide, and chloride) in a low-toxic and eco-friendly manner. The aim was to develop Pb-free perovskite materials that are less hazardous for workers in the photonics industry and that can be produced using inexpensive and less complicated processes. In this regards, a hydrophobic phenylammonium cation ( $[(C_6H_5)NH_3]^+$ ) was selected, which is known to contributed to a better sample stability. The synthesis methods involved three different approaches: one step solvent (OSS), OSS added oleic acid (OA), and a non-coordinated solvent method at different temperatures. The stability of the samples were evaluated, and it was observed that the ones synthesized at 60 °C exhibited the best stability for most of the solvents and types of halides. The strong ionic interaction between the  $BiX_6^{3-}$  anion and the short short  $PhA^+$  cations in the 0D structure greatly contributed to its stability. In general, the  $PhA_4BiCl_6$  sample showed the highest stability among the halides due to the stronger attraction between nucleus and electron. The study also involved the growth of a single crystal of  $PhA_4BiI_6$  using a solvent evaporation technique from which the structure of the zero-dimensional (0D) perovskite compounds was determined, supported by field emission scanning electron microscopy with energy-dispersive X-ray (FESEM-EDX) and Fourier transform infrared (FTIR) spectroscopy results. Microscopy techniques such as high-resolution transmission electron microscopy (HRTEM) and atomic force microscopy (AFM)

used to analyze the structure revealed QDs with sizes less than 10 nm. The energy bandgap varied among the halide samples, making them suitable for photonics applications such as LED, lasers, and other devices. The samples exhibited different peak emissions and transparency windows, making them suitable for various applications in lighting and photonics. The nonlinear optical properties were studied using z-scan measurements, and the samples showed a self-defocusing and reverse saturable absorption (RSA) phenomena. The larger the size of  $\text{PhA}_4\text{BiX}_6$  perovskites (from Cl to I-based), the stronger nonlinear refraction (NLR) indicated by a higher magnitude of  $n_2$  and  $\text{Re } \chi^{(3)}$ . Furthermore, the samples demonstrated optical limiting (OL) behaviour, with linear absorption followed by nonlinear extinction beyond a threshold. The OL mechanism was identified as energy spreading with self-defocusing mechanisms that is supported by the thermal nonlinear scattering on the QDs particles which arises from the continuous wave laser interaction. The  $\text{PhA}_4\text{BiI}_6$  sample showed the highest OL threshold power and was considered a promising and safe material for high-power laser applications and biological imaging. Overall, the synthesized perovskite materials show potential for applications in nonlinear photonics platforms, light sources, detectors, phosphors, and OL, particularly in advanced biological imaging techniques that require non-toxic substances.

# CHAPTER 1

## INTRODUCTION

### 1.1 Perovskites as nonlinear optical material

The field of photonics is becoming increasingly important nowadays, and the advancement of photonics materials is the main enabler of this. Engineered photonics nanomaterials such as fullerenes (Sergiy and Zynaida, 2017), carbon nanotubes (Chu *et al.*, 2020), and perovskite (Wang *et al.*, 2023), among many others, are being developed in collaboration with nanotechnology. Lately, researchers have been interested in synthetic perovskite because of its remarkable optical and electrical capabilities. Perovskite which bears Russian mineralogist Lev Perovski's name has a cubic structure identical to that of the mineral perovskite calcium titanate ( $\text{CaTiO}_3$ ), which has the formula  $\text{ABX}_3$ . The perovskite system is classified into two types: halide perovskites and inorganic oxide perovskites, which are each specifically designed for photovoltaics and energy applications, respectively (Hoye *et al.*, 2022). These perovskite can be engineered by combining the larger size 'A' atom with monovalent cations or alkaline earth metal cations, the 'B' atom with divalent alkaline metal group II (e.g., lead (Pb)), and the 'X' atom with oxygen or halide anions (fluoride, iodide, chloride, and bromide) (Aïssa *et al.*, 2021). Where, an A-site cation located on the corners of the lattice, B-site cations at the centre of the lattice, and X-site anions at the centre of the faces, forming an octahedron with the central B-site cation (VanOrman and Nienhaus, 2021).

Due to the low cost of preparation and the great degree of structural alteration that provides a rich playground for field researchers, halide perovskites have received substantial interest in recent decades. As a result of halide substitution, it feature a long and balanced diffusion length as well as bandgap tunability (Xu *et al.*, 2020). These

exceptional properties enable a wide range of more advanced nanophononics devices and applications apart from next-generation photovoltaics, such as photodetectors (Dong *et al.*, 2017), optical devices (Yamada *et al.*, 2020), light emitting diodes (Wang *et al.*, 2023) , and lasers (Zhou *et al.*, 2016). Besides that, due to their direct band gap (Xu *et al.*, 2020), high quantum efficiency (Chiba *et al.*, 2018), mild exciton binding energy (Lan *et al.*, 2019), high absorption coefficient (Ferrando *et al.*, 2018), and strong nonlinear response (Mirershadi *et al.*, 2016), halide perovskites have lately been regarded as having a promising potential for nonlinear photonics materials.

Halide perovskites exhibit optical absorption peak and absorption coefficient close to the band edge, greater than  $10^4 \text{ cm}^{-1}$ . By adjusting its size and dimension and substituting the halide, halide perovskite emission may span the full visible spectrum. However, for sufficiently high intensities, understanding the linear dielectric function, or alternatively, understanding the linear susceptibility, is insufficient to properly explain the system. At this point, it is important to explore the field of nonlinear optics (NLO) (Ferrando *et al.*, 2018). NLO is a rapidly growing field of research that is driving the development of novel materials and devices across a wide range of applications. Consequently, it is regarded as a pivotal element in the future of photonics technology. Figure 1.1 shows the trend of increased publication of NLO studies from 2015 to 2023, which indicates the importance of perovskite in the field of NLO. NLO is the branch of optics that describes the behaviour of light in nonlinear matter. The typical family of Pb-halide perovskites has received a lot of focus in terms of nonlinear behaviour (e.g.,  $\text{CH}_3\text{NH}_3\text{PbX}_3$ ) due to the abundance of theoretical and experimental research on this subject (Shen *et al.*, 2021). Bulk three-dimensional (3D)  $\text{CH}_3\text{NH}_3\text{PbBr}_3$  (Walters *et al.*, 2015) and  $\text{CH}_3\text{NH}_3\text{PbI}_3$  (March *et al.*, 2016) halide perovskite single crystals have been shown to have a strong nonlinear responses. Since



the discovery of 3D perovskites, low-dimensional perovskites materials ranging from 2D, 1D, and 0D, such as quantum wells, nanowires, have shown unexpectedly compelling nonlinear responses because of their potent quantum confinement (Lu *et al.*, 2016), amazing exciton effect (Wang *et al.*, 2021a), and structural variety (Zhou *et al.*, 2020).

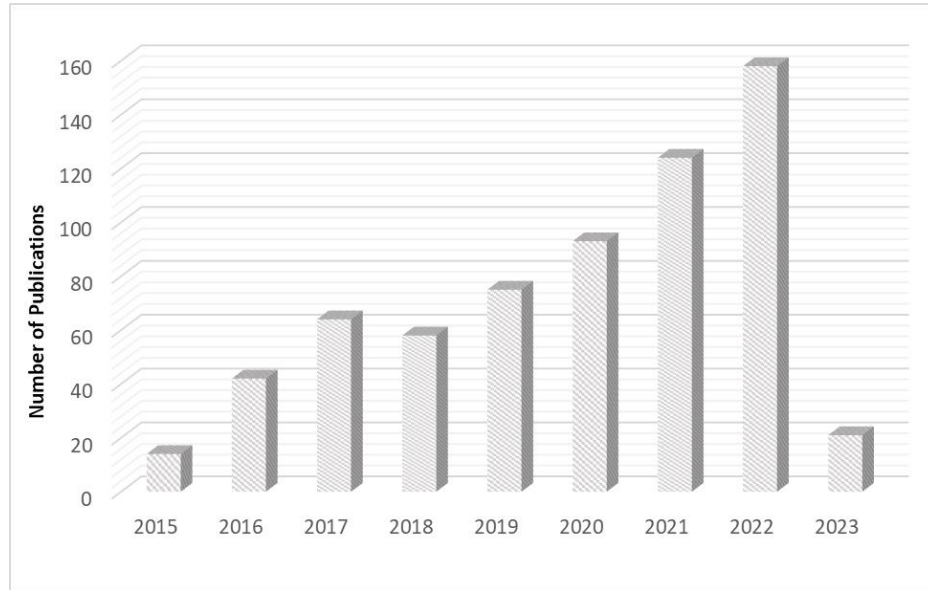


Figure 1.1 NLO study of perovskite publications for the past 8 years. Searched terms: " perovskite " and "nonlinear optics " (Source: Web of Science Core Collection only from January 2015 to February 2023).

Figure 1.2 illustrates the global NLO materials market for both second-order nonlinearity and third-order nonlinearity products, with an estimated value expected to reach USD 7110.09 million by 2027. These materials find applications in the electronics, automotive, and aerospace sectors. Understanding the NLO response of a material is crucial in unveiling its potential for optical devices and various applications. There are remarkable and unique ranges of NLO materials being explored such as chalcopyrite (Wang *et al.*, 2022), phthalocyanines (Biyiklioglu *et al.*, 2019), chalcogenides (Pradhan *et al.*, 2019), graphene (Al-Asadi *et al.*, 2019), black phosphorus (Zhang *et al.*, 2016a), hexagonal boron nitride (Caldwell *et al.*, 2019),

metal oxides (Boltaev *et al.*, 2019), metal halides (Gong *et al.*, 2019); and including perovskites for different applications.

Research on the low-dimensional structure of perovskite materials has been a growing area of interest in the scientific community in recent years. These modified structures can exhibit unique properties that are not observed in bulk perovskites, such as improved charge transport (Lin *et al.*, 2020), tuneable band gaps (Chouhan *et al.*, 2020), and enhanced optoelectronic properties (Zhu and Zhu, 2020). As such, perovskite quantum dots (QDs) were also discovered as a promising candidate for active laser media such as micro-photonics structures like micro-disk and micro-ring plasmonic lasers due to their high optical gain and photoluminescence quantum yields (Kamal *et al.*, 2021; Xing *et al.*, 2021; Stylianakis *et al.*, 2019). Maćzka *et al.* (2021) found several nonlinear optical phenomena, including second-harmonic generation, third-harmonic generation, two-photon excited luminescence, and multiphoton excited luminescence presented in a 2D perovskite compound. The creation of a 1D chiral amine-substituted hybrid Pb halide perovskite was reported by Yuan *et al.*, (2018) and Zhao *et al.* (2021) to disrupt the perovskite's centrosymmetric and achieve second-order nonlinear effects. Various review papers have been written to summarize the nonlinear performance of various structures of halide perovskite, as well as envisioned the future developments in halide perovskite photonics (Ferrando *et al.*, 2018; Xu *et al.*, 2020; Wang *et al.*, 2021a) especially Pb-based halide perovskite materials.

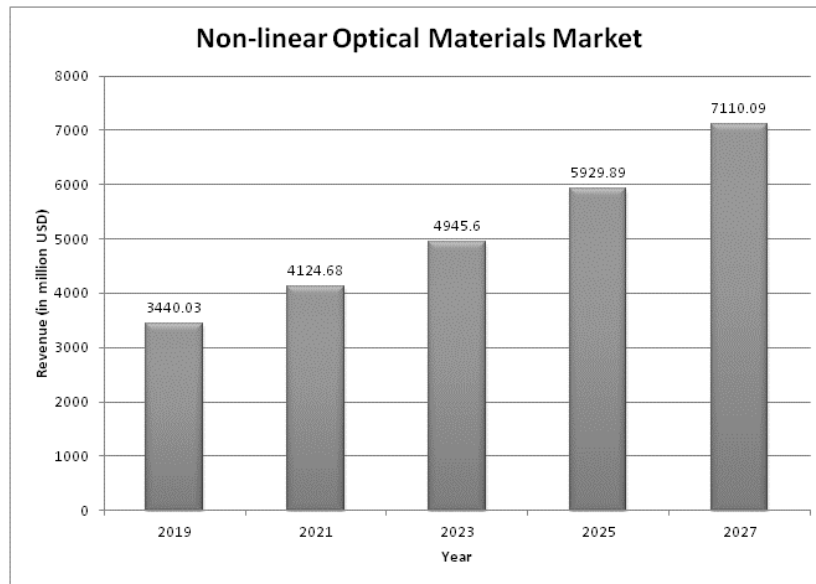


Figure 1.2 Nonlinear optical materials market by product type (second order nonlinearity and third order nonlinearity) for electronics, automotive and aerospace applications from 2019-2027 (Profshare Market Research, 2019).

## 1.2 Problem Statements

The increasing demand for advanced photonics technologies, which now extends into the realm of quantum technologies, substantiate the need to explore innovative materials for nonlinear optics (NLO) applications (Heshami *et al.*, 2016). This urgency arises from the critical requirement for materials that not only enhance device performance but also has broader spectral range effectively meeting the diverse demands of modern optical systems (Liu *et al.*, 2017d). The growing technological advancement underscores the necessity for materials that can unlock new frontiers in photonics, including applications in optical limiting (OL) (Sirleto and Righini, 2023).

This necessitates a deliberate focus on materials capable of pushing the boundaries of device performance, thus contributing to the seamless integration of advanced optical systems into diverse applications, from telecommunications to medical imaging (Ge *et al.*, 2021). Moreover, the global shift toward environmental awareness and sustainability underscores the importance of selecting materials that

align with eco-friendly principles. The materials under scrutiny should present an environmentally responsible option. The user-friendly fabrication not only simplifies the entire manufacturing process but also reduces its environmental footprint. This makes these materials the preferred option for achieving not only efficiency and scalability but also sustainable practices in the domain of photonics technologies (Jabbour *et al.*, 2018).

Hence, it is crucial to address the specific challenge of OL for laser protection, safeguarding human eyes, photodetectors, and sensors. The increased research of Pb-based perovskites in photonics industries for various types of photonics devices in recent years has been attributed to their comparatively straightforward and affordable manufacture employing solution-based processing methods, making them attractive for large-scale manufacturing. However, there are still some challenges that need to be addressed, such as stability issues and toxic concerns, before perovskites can be widely adopted in commercial photonics applications (Zhang *et al.*, 2018). The hazardous Pb that escaped from the deformed perovskite devices endangers the environment and people, bringing the attention of authorities (Liang and Gao, 2018). Moreover, workers and operators in the photonics production plant or factory who are exposed to Pb at a certain level will also be affected with Pb toxicity.

The European Union had regulated the restriction quantity of Pb in RoHS 3 compliance (EU Directive 2015/863) to less than 1000 ppm in electrical and electronic products (European Commission, 2015; Fan *et al.*, 2019). Many other countries expected to introduce similar regulations soon in future (Zhang *et al.*, 2017b). Meanwhile, Department of Occupational Safety and Health (DOSH) in Malaysia also enforce all factories in which any Pb process is used to compliance with the Factories and Machinery (Lead) Regulations 1984 and Occupational Safety and Health (Use and

Standards of exposure of Chemicals Hazardous to Health) Regulations 2000 to protect the safety of human and environment.

Therefore, it becomes essential to determine the optimum stability solution for long-lasting positive effects for Pb-based materials. Recently, researchers are attracted to explore highly stable perovskite materials which have excellent potential in photonics applications, including OL. Some researchers employ an encapsulation approach to shield against Pb or substitute Pb with non-toxic metal cations (Wei and Lin, 2018; Li *et al.*, 2021). Examples of these metal cations encompass tin (Sn), germanium (Ge), antimony (Sb), and bismuth (Bi). Some researchers have also found that low-dimensional perovskite structures exhibit superior stability compared to their bulk-size counterparts (Brichkin and Razumov, 2016; Han *et al.*, 2022).

While aiming to explore stable Pb perovskite materials or substitute Pb with low-toxic metals, it is important to ensure that the resulting materials retain their original promising properties, including their effectiveness in OL applications. Notably, perovskite materials hold the potential to drive advancements in NLO technology and industrial applications, particularly in the context of optical protection. Thus, it is imperative for all stakeholders to make substantial efforts in the exploration of novel, safe, and dependable NLO materials.

### **1.3 Research Questions**

In this study, we aim to answer these questions:

1. What are the effects of different solvents and temperatures on the stability of organic-inorganic Bi-halides perovskites, and what are the optimal conditions for their synthesis?

2. What is the crystal structure and particle size of the synthesized organic-inorganic Bi-halides perovskites?
3. What are the potential photonics applications arising from the linear optical properties and nonlinear optical behavior of the new synthesized organic-inorganic Bi-halide perovskites?
4. What is the underlying optical limiting (OL) mechanisms behind the optical effects observed in the synthesized organic-inorganic Bi-halide perovskites?

#### **1.4 Research Objectives**

The primary objective of this research is to synthesize Pb-free perovskites for environmentally sustainable photonics applications while also utilizing a less complex synthesis route. To accomplish this goal, several specific objectives have been identified:

1. To determine the optimum condition to synthesize organic-inorganic Bi-halide (iodide, bromide, and chloride) perovskites using various solvents and temperatures for the longest stability of the perovskites.
2. To perform structural and size characterization of the synthesized organic-inorganic Bi-halides perovskites.
3. To investigate the linear optical properties, luminescence, and nonlinear optical behaviour of the synthesized organic-inorganic Bi-halides perovskites.
4. To evaluate the OL performance and explore the mechanisms of the synthesized organic-inorganic Bi-halides perovskites.

#### **1.5 Novelty of the research work**

Li *et al.* (2019a) work inspired this research project. They successfully created a low-toxic phenylammonium bismuth iodide (PhABiI<sub>4</sub>) perovskite film that was

stable for 330 days by mixing hydroscopic phenylammonium iodide (PhAI) and bismuth (III) iodide ( $\text{BiI}_3$ ) in eco-friendly ethanol solvent and dried using gas pump treatment. Based on their work, we further explored the scope into few areas which provide the novelty of this research work as follows:

1. The single crystal perovskite of phenylammonium bismuth iodide ( $\text{PhA}_4\text{BiI}_6$ ) was presented, which yet to be reported in The Cambridge Crystallographic Data Centre. Based on the chemical formula, the perovskite in this research possesses a zero-dimensional structure.
2. The stability study by monitoring UV-vis absorbance spectra, optical properties and NLO responses of  $\text{PhA}_4\text{BiI}_6$  colloidal QDs are presented in this research.
3. Besides, the stability and NLO study of phenylammonium bismuth bromide ( $\text{PhA}_4\text{BiBr}_6$ ) and phenylammonium bismuth chloride ( $\text{PhA}_4\text{BiCl}_6$ ) colloidal QDs is also presented in this research, which has yet to be reported.
4. This work attempted to adopt an eco-friendly solvent, ethanol, to synthesise the perovskite nanomaterials; however, because the chloride sample reagent would not dissolve in ethanol between 25 °C and 100 °C, dimethyl sulfoxide is used instead. This study reduces the use of hazardous solvents and reagents and employs low-temperature synthesis in an ambient laboratory environment.

## **1.6 Research Scope**

The first part of this research reports the stability of low-dimensional organic Bi-based halides (iodide, bromide, and chloride) perovskite. The study is limited to three types of methods for synthesising each of the Pb-free halide QDs colloidal

solution samples by mixing PhA halides with Bi-based halides, which included one-step solvent (OSS), OSS added ligand, and non-coordinate solvent at three different setting temperatures of 25 °C, 60 °C, and 100 °C. UV-vis peak absorbance is used to monitor the stability of each sample and to determine the bandgap energy,  $E_g$ . Single crystal X-ray diffractometer (SC-XRD) is used to identify the structural of the single crystal organic Bi-based iodide. Meanwhile, Fourier transform infrared spectroscopy (FTIR), field emission scanning electron microscopy with energy dispersive x-ray spectroscopy (FESEM-EDX), high-resolution transmission electron microscopy (HRTEM), atomic force microscopy (AFM), and X-ray powder diffraction (XRD) are used to analyse the structure and size of the OSS samples. UV-vis spectroscopy, photoluminescence (PL) spectroscopy and luminescence chromaticity are used to study the optical properties of OSS added ligand samples. Meanwhile, NLO characterization of each sample is carried out using z-scan technique. The OL behaviour was characterized using modified open aperture z-scan setup.

## **1.7 Thesis outline**

The thesis comprises of five main chapters.

Chapter 2 covers an introduction to the thesis topic as well as a literature review. The literature flow starts with an overview of NLO and then moves on to the discussion about traditional NLO materials. Following that, the advantages of Bi-based halide perovskites and QDs perovskites as NLO materials are explained as well as the fundamental drawbacks of prototypical family Pb-based halide perovskites. The previous research important achievements, as well as the suggestions for synthesising and issues dealing with the hybrid perovskites, were also assessed.



Chapter 3 described all the substances and equipment utilised in this study, as well as the technique employed to conduct the research. It also explains how to prepare the precursor solution, colloidal solution, solid-form samples, and single crystal. This chapter also covers characterization techniques for studying the optical properties, structural and NLO responses of samples.

The findings of the experiments are presented and discussed in Chapter 4. The results of each characterization were inspected and assessed. This covers the performance of stability, optical properties, structural and size characterization, NLO properties, and OL performance.

Chapter 5 evaluated the findings and provided an overview of the study accomplishments. Finally, a few suggestions for future study related to these hybrid Bi-based halide perovskites are proposed.

## CHAPTER 2

### LITERATURE REVIEW AND THEORY

#### 2.1 Introduction

This chapter provides a comprehensive review of prior research on halide perovskite materials and the methods employed in preparing nonlinear optics (NLO) materials, which serve as the foundation for this study. The fundamentals of NLO theory are also presented. The insights gained from this literature review have inspired and guided this research efforts towards exploring low-cost, low-hazard, and lead (Pb)-free hybrid organic-inorganic metal halide perovskite nanomaterials. These materials hold significant promise for potential integration into future photonics technologies.

#### 2.2 Halide Perovskite – three-dimensional (3D) - zero-dimensional (0D)

Perovskite was discovered in 1839 as an exceptionally adaptable crystal structure alkaline element ( $\text{CaTiO}_3$ ) mineral initially found on Earth and a popular subject for cutting-edge scientific research. This mineral which located 2600 km down the earth in lower mantle is denser and mechanically weak but has a high electrical conductivity. Synthetic perovskite can be obtained just by mixing two inexpensive salts, Pb halides and organic halides. The solution forms can be spin-coated to produce a thin uniform layer of application. The general formula of perovskite  $\text{ABX}_3$ , composed of five atoms per unit cell, where A and B are the alkaline earth metal cations and 'X' is anion as shown in Figure 2.1 (Tan *et al.*, 2014). Monovalent cation "A" is located at a corner, and metal cation "B" metal group II (divalent) which smaller than 'A' is located at the centre, and anion "X" located at the centre of six planes consist of anionic frameworks of corner sharing B–X octahedra. Perovskite crystalline system can be divided into two group inorganic oxide perovskite and halide perovskite.

Inorganic oxide consists of intrinsic and doped perovskite which mainly used in ferroelectric, piezoelectric and pyroelectric applications. Meanwhile, halide perovskite consists of organo-metal and alkali types of perovskites which mainly specifically designed for photovoltaics (Hoye *et al.*, 2022).

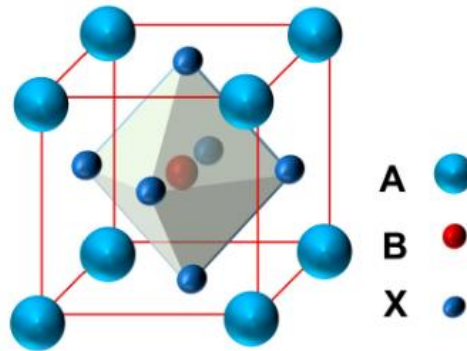


Figure 2.1 Single unit cell of an ABX<sub>3</sub> perovskite crystal (Tan *et al.*, 2014).

Hybrid halide perovskites are a group of substances having the chemical formula A<sub>x</sub>M<sub>y</sub>X<sub>z</sub> (x, y, and z depend on the structural dimensionality), where A is an organic or inorganic cation, M is a metal cation, and X is a halide anion (I/Br/Cl). Figure 2.2 shows examples of the hybrid perovskite's varied crystal forms. The perovskite structures can incorporate ions of various size and charge showing great flexibility of composition to substitute various size of cation A moieties and any type of metal B moieties to form into different morphologies, such as thin films, single crystals, microcrystals, or nanocrystals (Xu *et al.*, 2020). 90% of the elements in the periodic table can be stable in the perovskite structure and the feasibility of partial substitutions of cations in A<sup>-</sup> and B<sup>-</sup> sites to form A<sup>1-x</sup> (Atta *et al.*, 2016). The substitutions of ions into the A<sup>-</sup> and B<sup>-</sup> sites, A<sup>-</sup> or B<sup>-</sup> sites or deviation from ideal stoichiometry will affect the electronic properties of the man-made perovskites.

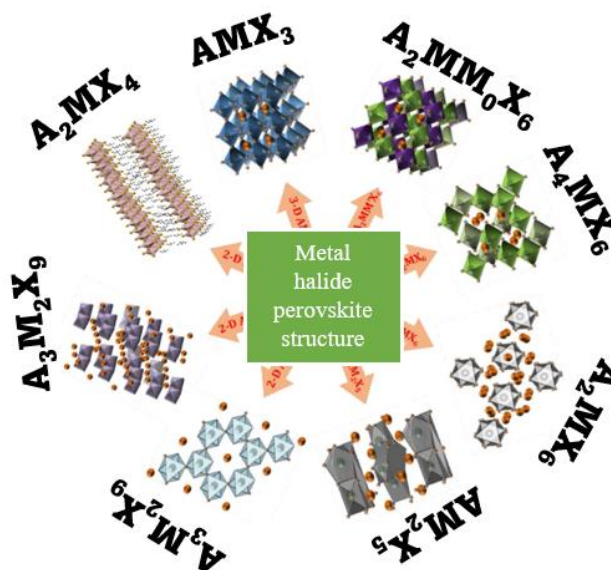


Figure 2.2 Different metal halide perovskite crystal structures of 3D cubic-phase  $AMX_3$ , 2D  $A_2MX_4$ , 2D  $A_3M_2X_9$ , 2D  $AM_2X_5$ , 0D  $A_4MX_6$ , and 3D double perovskites  $A_2MM_0X_6$  (Bhaumik *et al.*, 2020).

For 0D nanomaterials with structural diameters ranging from 1 to 20 nm, there are no network connecting octahedra. The formation of bulk materials with structural diameters over 20 nm consists of a network over one axis for 1D, a network over two axes for 2D, and a network over three axes for 3D (González-Carrero *et al.*, 2015). Figure 2.3 shows the standard-perovskites (3D), 2D perovskites with various types of layer chains of octahedra in 1D perovskites, discrete octahedra separated by organic cations (0D), and perovskite-like halides with moieties of edge- and face-sharing octahedra. (Song *et al.*, 2019). Thus, the electronic energy bands of perovskites and layered perovskites are quite unusual, and their structure has features that are unique.

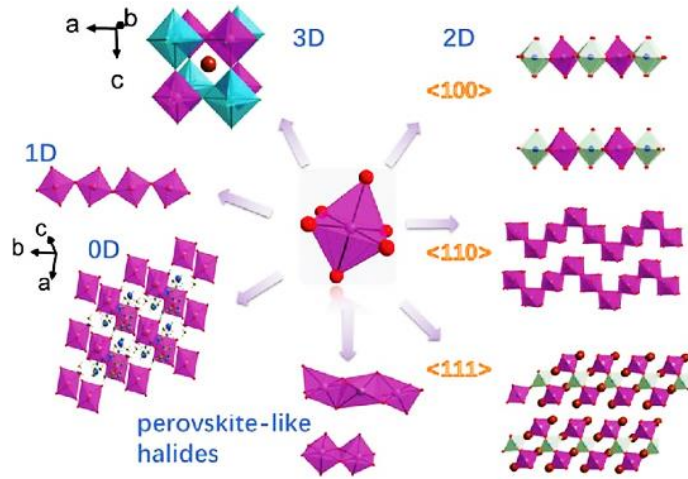


Figure 2.3 Types of connectivity  $BX_6$  octahedra in perovskite-like halides (Song *et al.*, 2019).

Perovskites have the advantage of being able to be synthesized and grown utilising solution-based, low-temperature processes. Due to the flexibility and ease of replicating the molecular structure of perovskite, different types of perovskites were studied, such as double perovskite, organic perovskite, hybrid perovskite, inorganic perovskite, metal perovskite, oxide perovskite, chalcogenide perovskites, and colloidal QDs crystals of perovskite (Atta *et al.*, 2016; Xiao *et al.*, 2018). As a result, it is simple to synthesise varied dimensionalities to improve moisture resistance. When compared to 3D perovskites, low-dimensional perovskites exhibit higher chemical stability. However, 3D types outperform low-dimensional types in terms of device performance (Chen *et al.*, 2021; Ju *et al.*, 2018). Perovskites in 1D and 0D have a low defect density, can tolerate lattice stresses, and can prevent material recombination and degradation.

Perovskite's electrical, optical, and magnetic characteristics performed well in switching, filtering, and surface acoustic wave signal processing devices. These material's electrical characteristics can be easily adjusted for several applications. Organic perovskites offer better ferroelectric characteristics than inorganic perovskites due to their vast range of chemical compositions from divalent organic cations (Stoddart, 2018). Inorganic perovskites commonly exhibit strong interactions through

covalent and ionic bonding, resulting in high electrical mobility, a wide range of band gaps, dielectric constants, and substantial mechanical and thermal properties. Hybrid perovskites comprise a combination of organic cations and metal halide anions that have greater physical and chemical characteristics than separate organic and inorganic compounds. This is owing to the impact of strong interactions in low-dimensional structures surrounded by both substances with a significantly lower dielectric constant. It possesses remarkable excitonic characteristics, extremely low thermal conductivity, and interesting new features (Seok and Guo, 2020; Garmire, 2013; Zhou *et al.*, 2018).

Kasel *et al.* (2019) discovered that metal-free perovskites and dipole moments from organic groups on the A cation had a significant impact on NLO characteristics. The ferroelectric domain of hybrid Pb halide perovskites have recently been confirmed by researchers, a property that appears to be connected to the presence of polar molecular cations in the crystalline framework. These ferroelectric domains may help in the separation of photoexcited electron-hole pairs as well as the reduction of charge carrier recombination. As a result, hybrid Pb halide perovskites are anticipated to have substantial optical nonlinearity, a notion that has recently been proven (Krasnok *et al.*, 2018; Grabowska, 2016). Due to their unique opto electronic properties, such as size tunable absorption and bandgap, high optical extinction coefficient, and multiple exciton generation characteristics, low-dimensional perovskite, with sizes ranging from 2 nm to 10 nm have recently received a lot of attention. Figure 2.4 depicts the increase in energy bandgap as the perovskite dimension decreases.

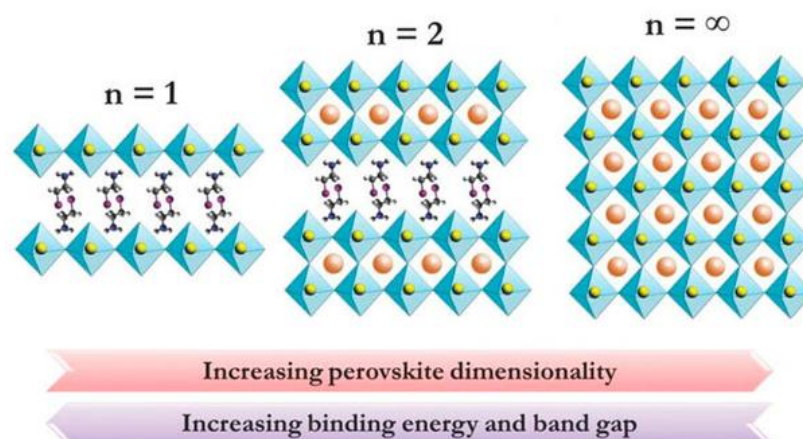


Figure 2.4 Energy band gap versus perovskite dimension (Han *et al.*, 2020).

Perovskites QDs exhibit nanoscale excitons and can be used in transistors, diode lasers, LEDs, and fluorescent biomedical imaging (Younis *et al.*, 2020). Owing to the significant inherent quantum confinement effects of 0D perovskite (3D confinement), limited carrier motility may occur, limiting solar efficiency (Edvinsson, 2018). Colloidal QDs with a quantized energy structure exhibit a unique nanoscale quantum confinement phenomenon along with a wealth of optics and characteristics. Figure 2.5 depicts the bandgap-related quantum confinement effects of 0D materials in comparison to other dimensional materials. For isolated octahedra, 0D perovskite has a higher exciton binding energy than 3D perovskite, effectively preventing exciton dissociation at ambient temperature. It is advantageous to photon-emitting optoelectronic devices. Because of the metal halide octahedron units are shielded by the organic shells, 0D organic metal halide perovskite exhibits extraordinary stability in the ambient environment (Sun *et al.*, 2021). QDs materials are also more resistant to moisture than bulk-size materials (Baig *et al.*, 2021). In a 3D structure, such as a bulk material, there is a lack of confinement in comparison to lower-dimensional structures. This absence of confinement means that the electrons and charge carriers within the material have more freedom to move in various directions. As a result, the

energy levels and electronic states become more spread out, leading to a lower bandgap (Edvinsson, 2018).

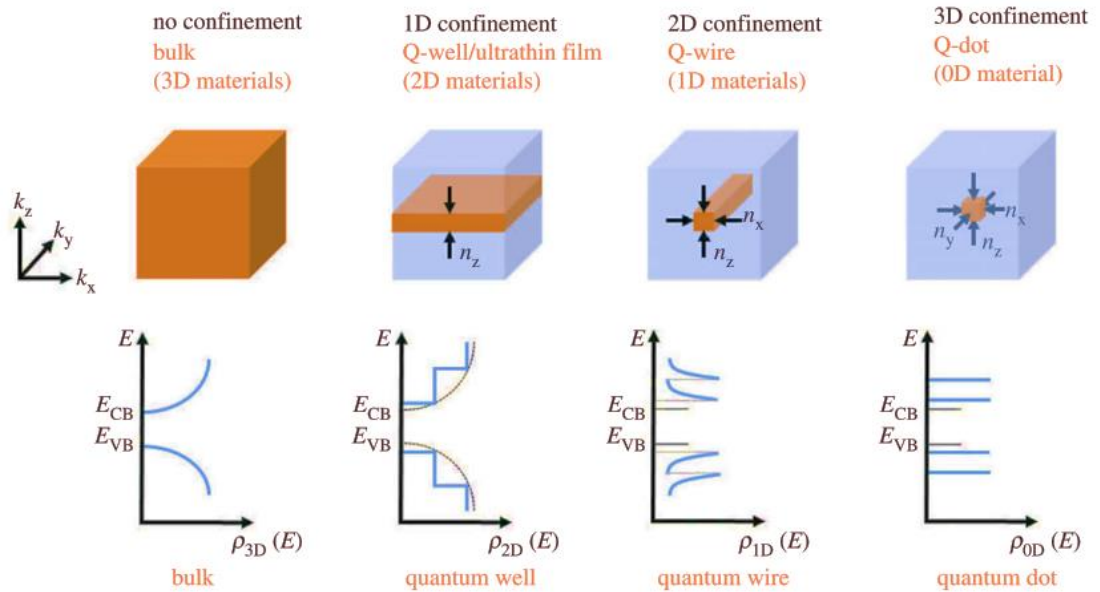


Figure 2.5 The degree of confinement for different structure of materials. (Edvinsson, 2018).

The separated octahedra in 0D perovskites prevent metal ion interactions and generate optical characteristics identical to the individual octahedra. The octahedra's isolation is projected to result in strong quantum confinement. Because of the energy levels within the crystal, different-sized QDs affect the colour emitted or absorbed by the crystal. Colour can also be adjusted using mixed halides. Moreover, the size of the dots has the greatest influence on the optical characteristics. Because of the small size of the dots and mixed halides, they can create nanocrystals with narrow emission linewidths. It possesses broad absorption, narrow emission, ultrafast carrier excitation-relaxation processes, and a size-tuneable band gap across a large energy range (Lu *et al.*, 2016). Perovskites have remarkable optical and electrical characteristics at zero degree of separation, including wavelength tunability, extended photocarrier lifetimes, long carrier diffusion lengths, high fluorescence yields, and ambipolar transport (Yin *et al.*, 2017). The usage of 0D perovskites in next-generation LEDs, lasers, and



photonics devices were studied (Zhu and Gong, 2021). 0D perovskites have proven high performance in novel photonics applications (Li *et al.*, 2017b).

In summary, halide perovskite materials have attracted researcher's attention in recent years due to their exceptional optoelectronic properties and versatility in various applications. The 3D perovskites have continuous structures and find use in high-efficiency solar cells and optoelectronic devices, but it faces stability challenges. In contrast, unique properties of 0D perovskites include size tunability, exceptional quantum yield, and solution processability. These features have made 0D perovskites promising candidates for displays and sensitive sensors, where precise control over the size and properties of nanocrystals is essential, particularly in the context of nonlinear optics. The future of halide perovskite research holds promise as scientists and engineers continue to explore the unique advantages of both 3D and 0D structures. Ongoing efforts aim to enhance the stability of 3D perovskites and unlock new applications for 0D perovskite nanocrystals.

### **2.3 Drawbacks of Perovskites**

Hybrid halide perovskite has attracted intensive research by scientists for photonics device applications, mainly regarding their remarkable photophysical properties that occur between organic and inorganic, as well as easy to synthesise at low temperatures (Haque *et al.*, 2019; Gong *et al.*, 2019). However, hybrid perovskites with a core Pb-based due to their instability in ambient environments when exposed to heat, oxygen, moisture, and light became the main obstacles for all (Shangguan *et al.*, 2020). The reason is caused by the weak hydrogen bonding between monovalent organic cations and octahedral  $\text{Pb}^{2+}$  (Wang *et al.*, 2018). Organic Pb-based perovskite solar panels face challenges related to stability, durability, and Pb concerns, making

their commercialization more difficult, despite their high efficiency in converting light into electricity. The toxic Pb substance will be released from the perovskite structure and threaten the environment and human life (Wei *et al.*, 2019a). Despite poor stability, several solutions for improving stability have been researched and implemented due to the remarkable features of the perovskite. Researchers discovered molecular instability, degradation, or breakdown in perovskites are due to interactions between ionic compounds and surface ligands, as well as long-term exposure to UV moisture, radiation, oxygen, heat, and humidity (Zuo and Ding, 2021; Nelson and Cochran, 2019; Xiao *et al.*, 2020). Figure 2.6 shows the perovskite stability issues that are listed down by Mazumdar *et al.* (2021).

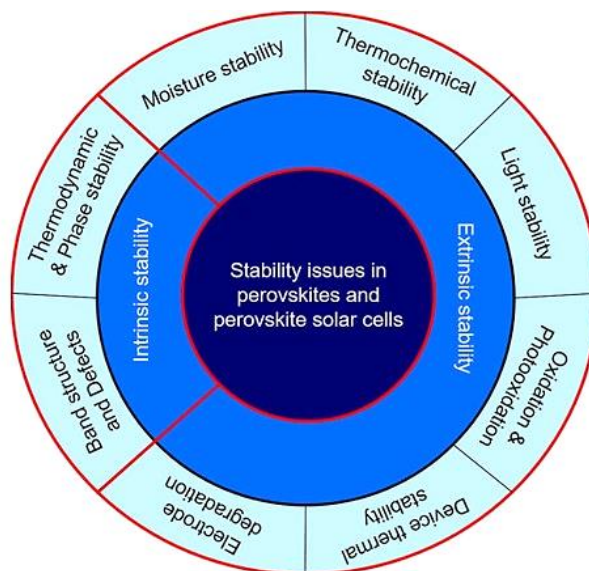


Figure 2.6 Stability issues in perovskites and perovskites solar cells (Mazumdar *et al.*, 2021).

The water solubility of Pb atoms may cause environmental pollution and harm to life on Earth. Therefore, it is crucial to develop a more robust Pb-free perovskite material to enhance stability for long-term beneficial impact (Chen *et al.*, 2021; Slavney *et al.*, 2017; Yang *et al.*, 2018). University of Groningen scientists found that the ability to form thin films and the structure of the materials for the solar cells were related to how Pb-free perovskite crystals form and how the crystal structure affects

the functioning of the solar cells (Dong *et al.*, 2020). Wei *et al.* (2019b), Lou *et al.* (2019) and Ahmadi *et al.* (2017) also identified the prospects and main future challenges for overcoming disadvantages and improving stability performance for future development into compositional engineering, fabrication technology (waterproof matrix encapsulation and device encapsulation), and surface engineering (interfacial optimization).

The manufacturing cost of Pb-free halide perovskite devices can be inexpensive because a molecular structure can be easily replicated in a cost-effective fashion for mass production of devices (Jerpoth *et al.*, 2020). This will pave the way for less hazardous nonlinear semiconductor materials in the future. Because the NLO and OL performances of these materials have been less studied thus far, new material breakthroughs will be required before the promise can become a reality, as the key problem in Pb-free halide perovskite research today is the lack of long-term stability and sensitivity to moisture in the open air. As of February 2023, Pb-free perovskite QD research is increasing since 2016, as indicated in Figure 2.7.

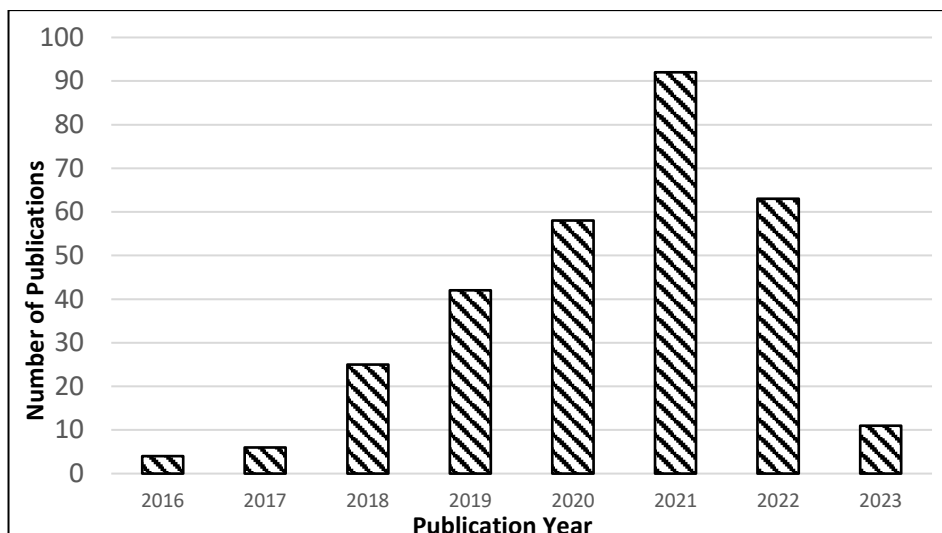


Figure 2.7 Pb-free Perovskite QDs publication. Searched terms: "perovskite", "quantum dot" and "lead-free " (Source: Web of Science Core Collection only from January 2016 to February 2023).

In summary, despite the remarkable promise exhibited by halide perovskite materials across diverse applications, it is imperative to acknowledge the existence of substantial challenges within this flourishing field. These challenges encompass the critical issues of stability, as perovskites are known to degrade under certain conditions, raising concerns of long-term performance and viability in practical applications. Furthermore, the need for continued research and innovation remains utmost to overcome these obstacles and optimize the performance, durability, and reliability of perovskite materials, ensuring full realization as a transformative technology.

#### 2.4 Toxicological research of lead (Pb) - based perovskite

Addressing the toxicological concerns associated with Pb-based perovskite materials is paramount for the advancement of photonic technologies. The contamination of the environment by Pb in perovskite materials poses significant health risks to both humans and animals, compounded by its cumulative toxicity (Handl, 2018). Studies have indicated that the presence of Pb in these materials can

potentially lead to cellular damage and subsequent health implications (Benmessaoud *et al.*, 2016). In response to these toxicological and regulatory concerns, researchers are actively seeking environmentally friendly alternative strategies to manage Pb-related issues. This is crucial to ensure the safety of both workers involved in manufacturing and end-users (Passini *et al.*, 2023).

Mitigating Pb contamination in perovskite materials, one of the methods involves chemisorption, a technique to prevent Pb from leaching out when the material is utilized by researchers to overcome the Pb issue. This technique involves the use of Pb-absorbing materials within or outside the device structure, including additives, hole-transporting layers, interfacial modifiers, and encapsulation layers (Wu and Zhang, 2022). Kojić *et al.* (2021) employed polyvinylpyrrolidone as a stabilizing additive to investigate its impact on the optical and electrical properties of perovskite formamidinium Pb iodide thin films. Their study successfully prevented film degradation even after aging for 2 months in an ambient atmosphere. Additionally, Tsai *et al.* (2015) demonstrated high-performance conventional hole-transport layer-free perovskite solar cells, facilitating effective charge extraction at the ITO/perovskite interface.

To enhance perovskite's stability, interfacial modifiers such as cesium compounds are integrated into the ZnO electron transport layer of perovskite solar cells. Mahmud *et al.* (2018) succeeded in showing that devices utilizing cesium acetate exhibited an impressive 400% enhancement in stability compared to conventional cesium carbonate devices. Even after a 30-day systematic degradation study, the cesium acetate devices retained nearly 90% of their initial power conversion efficiency. Li *et al.* (2022) developed a cost-effective encapsulation technique using commercial cation exchange and UV resins to protect both rigid and flexible

perovskite solar cells. This approach efficiently captures leaked  $\text{Pb}^{2+}$  from degraded perovskites, ensuring enhanced performance.

Moreover, recycling and sustainable practices, Binek *et al.* (2016) addressed the recycling of Pb-based perovskite devices by incorporating disassembly to recover valuable materials while minimizing Pb exposure. Efficient separation methods reclaim Pb and other components for reuse, and advanced extraction techniques isolate Pb and other valuable elements, reducing resource waste. Comprehensive recycling diminishes the environmental impact of Pb contamination, and repurposing recycled Pb materials minimizes the need for virgin resources and energy-intensive extraction, thereby fostering a sustainable, closed-loop lifecycle for perovskite materials (Ravi *et al.*, 2020).

Furthermore, transitioning to safer, Pb-free perovskites alternatives represents a pivotal shift in advancing the environmental and health aspects of perovskite technology (Schileo and Grancini, 2021). Embracing Pb-free perovskite materials aligns the industry with evolving safety standards and contributes to the development of cleaner and safer energy technologies. However, research suggests that the similar harmful effects observed in lab tests with lead iodide ( $\text{PbI}_2$ ) and tin iodide ( $\text{SnI}_2$ ) indicate that switching from Pb to Sn might not be a favorable solution. Bismuth could be a more promising choice to replace Pb in terms of eco-friendliness, although materials using bismuth have limitations when it comes to making solar cells (Chetyrkina *et al.*, 2023).

In summary, the toxicological investigation of Pb-based perovskite materials represents a critical aspect of this research area. This comprehensive analysis has unveiled potential environmental and health concerns raising questions about the long-term safety and sustainability. Through rigorous experimentation and evaluation, this